Earth and Planetary Science Letters 298 (2010) 244–254

Contents lists available at ScienceDirect

Earth and Planetary Science Letters

journal homepage: www.elsevier.com/locate/epsl

The release of ^{14}C-depleted carbon from the deep ocean during the last deglaciation: Evidence from the Arabian Sea

Sean P. Bryan *, Thomas M. Marchitto, Scott J. Lehman

Institute of Arctic and Alpine Research and Department of Geological Sciences, University of Colorado, Campus Box 450, Boulder, CO 80309-0450, USA

ARTICLE INFO

Article history:
Received 7 June 2010
Received in revised form 19 August 2010
Accepted 20 August 2010
Available online 6 September 2010

Editor: P. DeMenocal

Keywords:
radiocarbon
deglaciation
Arabian Sea
intermediate water
AAIW
carbon cycle

ABSTRACT

During the last deglaciation the concentration of CO_2 in the atmosphere increased and the radiocarbon activity ($\Delta^{14}C$) of the atmosphere declined in two steps corresponding in timing to Heinrich Stadial 1 and the Younger Dryas. These changes have been attributed to the redistribution of ^{14}C-depleted carbon from the deep ocean into the upper ocean and atmosphere. Recently, reconstructions of $\Delta^{14}C$ in intermediate waters of the eastern tropical Pacific have revealed pulses of very old water during the deglaciation, consistent with the release of ^{14}C-depleted carbon from the deep ocean at this time. Here, we present reconstructions of intermediate water $\Delta^{14}C$ from the northern Arabian Sea near the coast of Oman. These reconstructions record significant aging of intermediate waters in the Arabian Sea during Heinrich Stadial 1 and, to a lesser extent, during the Younger Dryas. The timing and magnitude of ^{14}C depletion in the Arabian Sea during Heinrich Stadial 1 is very similar to that previously observed in the eastern North Pacific near Baja California, indicating that similar mechanisms were involved in controlling $\Delta^{14}C$ at these two sites. The most parsimonious explanation of the $\Delta^{14}C$ records from the Arabian Sea and Baja California remains the release of ^{14}C-depleted carbon from the deep ocean by renewal of upwelling and mixing in the Southern Ocean. These ^{14}C-depleted waters would have been incorporated into thermocline and intermediate water masses formed in the Southern Ocean and spread northward into the Pacific, Indian and Atlantic Ocean basins.

1. Introduction

During the last glacial termination (~18–10 kyr BP) the concentration of CO_2 in the atmosphere increased by ~50% in two steps corresponding in timing to Heinrich Stadial 1 (HS1) and the Younger Dryas (YD) (2001). Most attempts to explain the CO_2 rise involve changes in the distribution of carbon between the atmosphere and the deep ocean, since the deep ocean is the largest reservoir of carbon that can interact with the atmosphere on relevant timescales (e.g., Archer et al., 2000; Broecker, 1982; Sigman and Boyle, 2000). However, the exact mechanisms involved remain unclear. At the same time as CO_2 was rising, the radiocarbon activity ($\Delta^{14}C$) of the atmosphere decreased rapidly (e.g., Fairbanks et al., 2005; Hughen et al., 2004, 2006; Marchitto et al., 2007; Reimer et al., 2004, 2009). The decline in atmospheric $\Delta^{14}C$ cannot be entirely explained by changes in ^{14}C production. Production of ^{14}C was elevated at times during the last glacial period due to lower geomagnetic field strength, particularly during the Laschamp and Mono Lake excursions (Laj et al., 2002; Muscheler et al., 2004). However, reconstructions of ^{14}C production based on paleomagnetic records and ^{10}Be in ocean sediments indicate only a small decrease during the deglaciation (Frank et al., 1997; Laj et al., 2002), and reconstructions based on ^{10}Be in the Greenland Summit ice cores indicate very little change (Muscheler et al., 2004). Broecker and Barker (2007) estimated that a maximum of about 37‰ out of the ~190‰ decrease in $\Delta^{14}C$ that occurred between ~17.5 kyr BP and ~14.5 kyr BP can be explained by ^{14}C production. These observations indicate that changes in the distribution of ^{14}C between the atmosphere and other carbon reservoirs must be responsible for much of the deglacial $\Delta^{14}C$ decline (Broecker and Barker, 2007; Hughen et al., 2004, 2006; Muscheler et al., 2004). This hypothesis requires that during the last glacial period, ventilation of some portion of the deep ocean (the only carbon reservoir large enough to explain the changes) was greatly reduced, allowing ^{14}C to decay away with limited renewal from the surface ocean. During the deglaciation, the ^{14}C-depleted carbon in this reservoir was mixed back into the rest of the ocean and atmosphere. The hypothesized isolated deep ocean reservoir may have been stabilized by very high salinity associated with sea ice formation and brine rejection in the Southern Ocean (Adkins et al., 2002). An isolated deep ocean reservoir may have also accumulated remineralized organic carbon, providing at least a partial explanation for the glacial–interglacial pCO_2 changes (Sigman and Boyle, 2000; Toggweiler, 1999; Watson and Naveira Garabato, 2006).

According to this hypothesis, the radiocarbon age of the isolated deep ocean reservoir should appear very old when compared to the contemporaneous atmosphere or surface ocean. While the extent of aged deep waters in the glacial ocean remains unclear, recent records

* Corresponding author. Tel.: +1 303 492 5792; fax: +1 303 492 6388.
E-mail address: sean.bryan@colorado.edu (S.P. Bryan).

0012-821X/$ – see front matter © 2010 Elsevier B.V. All rights reserved.
doi:10.1016/j.epsl.2010.08.025

have provided increasing evidence that some portion of the glacial deep ocean was very poorly ventilated. There is strong evidence that the glacial North Atlantic was significantly depleted in ^{14}C relative to the modern North Atlantic. Benthic–planktic foraminiferal age differences indicate that the glacial North Atlantic below 2.5 km was ~200–300‰ lower than the contemporaneous atmosphere (Keigwin, 2004; Keigwin and Schlegel, 2002; Robinson et al., 2005; Skinner and Shackleton, 2004). These measurements are consistent with a glacial Atlantic in which North Atlantic Deep Water (NADW) was a shallower water mass and deep waters sourced from high southern latitudes (hereafter southern source) filled the ocean below ~2500 m (cf. Curry and Oppo, 2005; Marchitto and Broecker, 2006), along with some additional aging of glacial southern source deep waters relative to modern. Recent work by Skinner et al. (2010) indicates that deep waters in the Atlantic sector of the Southern Ocean were ~470–520‰ lower than the atmosphere during the last glacial maximum. However, results from the Pacific have generally shown deep ocean ^{14}C depletions similar to or only slightly greater than today's (W. Broecker et al., 2004; W.S. Broecker et al., 2004; Broecker et al., 2007, 2008; Galbraith et al., 2007; Shackleton et al., 1988), suggesting that the old reservoir was rather limited in spatial extent. One study, which used volcanic tephras as stratigraphic markers, has found glacial deep waters in the southwest Pacific that were ~300–500‰ lower than the atmosphere (Sikes et al., 2000). There is also some unpublished data indicating substantial ^{14}C depletion in waters below 3 km in the Eastern Equatorial Pacific (EEP) (Keigwin et al., 2006). The lack of consensus regarding the ^{14}C content of the deep ocean in the past may be due in part to low sedimentation rates, poor carbonate preservation, and bioturbation, all of which typify deep ocean sediments (Barker et al., 2007; Peng and Broecker, 1984).

Compelling evidence for a ^{14}C-depleted carbon reservoir in the glacial ocean was presented by Marchitto et al. (2007) using a reconstruction of $\Delta^{14}C$ in intermediate waters near Baja California. The Baja California record shows two pulses of extremely old waters during the deglaciation that coincide in timing with the decreases in atmospheric $\Delta^{14}C$ and the increases in atmospheric pCO_2. Marchitto et al. (2007) proposed that the ^{14}C-depleted carbon must have been sourced from an isolated deep ocean water mass. Given the strong similarity between the timing of the deglacial carbon cycle changes and warming in Antarctica and the Southern Ocean, Marchitto et al. (2007) suggested that the old carbon was upwelled in the Southern Ocean and advected to the Baja California margin via Antarctic Intermediate Water (AAIW) and/or Subantarctic Mode Water (SAMW). The recent reconstruction of deep Southern Ocean ventilation age by Skinner et al. (2010) confirms that this ocean could have supplied old water to the upper ocean and atmosphere, but the extent of aging was still somewhat lower than required to explain the observations of Marchitto et al. (2007). If the old carbon observed at Baja California was indeed sourced from an isolated deep ocean water mass and upwelled in the Southern Ocean during the deglaciation, the depleted $\Delta^{14}C$ signal should also be recorded in intermediate depth cores from other regions that are influenced by AAIW and SAMW. In this paper we test this hypothesis using sediment cores from intermediate depths in the Arabian Sea.

2. Arabian Sea study site

Our new measurements come from two sediment cores collected in the northern Arabian Sea near the coast of Oman: RC27-14 and RC27-23 (Table 1; Fig. 1). These cores were selected for two primary reasons: they contain stratigraphic information that can be used to develop age models that are independent of ^{14}C, and we expect that they would have been influenced by SAMW or AAIW during the deglaciation. The core sites sit within a strong oxygen minimum zone related in part to monsoon-driven coastal upwelling. Previous work on these sediment cores demonstrated that the $\delta^{15}N$ of organic matter, which is influenced by denitrification in the water column, displays clear evidence of Dansgaard–Oeschger cycles and can therefore be correlated with $\delta^{18}O$ records from the Greenland ice cores (Altabet et al., 2002). This relationship is mechanistically tied to the strength of the Southwest Indian Monsoon. On millennial timescales warmer Northern Hemisphere high latitudes correspond to a stronger Southwest Indian Monsoon (e.g., Burns et al., 2003; Fleitmann et al., 2003; Sinha et al., 2005). Stronger monsoons drive increased upwelling and productivity in the northern Arabian Sea, increasing oxidant demand, and increasing denitrification (Altabet et al., 2002; Ganeshram et al., 2000; Ivanochko et al., 2005; Schulz et al., 1998). ^{14}N is preferentially removed during water column denitrification, leaving the remaining nitrogen pool and the organic matter that incorporates it enriched in ^{15}N (Brandes et al., 1998; Cline and Kaplan, 1975).

We apply the GISP2 calendar age model (Meese et al., 1997) to RC27-14 and RC27-23 by correlating the $\delta^{15}N$ records from the two sediment cores to the GISP2 $\delta^{18}O$ record (Grootes and Stuiver, 1997). To do this, we established five tie points between the sediment cores and GISP2 and used a linear interpolation in between the tie points (Fig. 2a). Since the Greenland-monsoon teleconnection is via the atmosphere, we assume that the transitions apparent in the $\delta^{15}N$ and the $\delta^{18}O$ records are synchronous within the resolution of the sediment cores. The resulting sedimentation rates range from 12.7 to 15.3 cm/kyr for RC27-14 and 10.5 to 13.0 cm/kyr for RC27-23. Error in our calendar ages was estimated using a Monte Carlo analysis including an estimated uncertainty in the placement of tie points of 200–500 yr and a 10% uncertainty in the sedimentation rate between the sample depth and the nearest tie point. This error analysis does not include possible error in the GISP2 age model. However, the strong agreement between the GISP2 age model and the U–Th-dated Hulu Cave speleothem record (Wang et al., 2001) during the deglaciation indicates that possible errors in the GISP2 age model are small (<~100 yr) during the time interval of interest here.

SAMW and AAIW ventilate much of the thermocline and intermediate waters of the Indian Ocean (McCarthy and Talley, 1999; Sloyan and Rintoul, 2001; You, 1998). These water masses are difficult to identify in the modern Arabian Sea due to mixing along

Table 1
Location of intermediate water $\Delta^{14}C$ sites discussed in this paper.

Location	Core	Latitude	Longitude	Water depth (m)	Reference
Arabian Sea	RC27-14	18.3°N	57.6°E	596	This study
Arabian Sea	RC27-23	18°N	57.6°E	820	This study
Baja California	MV99-MC19/GC31/PC08	23.5°N	111.6°W	705	Marchitto et al. (2007)
Eastern Equatorial Pacific	VM21-30	1.2°S	89.7°W	617	Stott et al. (2009)
Chile Margin	SO161-SL22	36.2°S	73.7°W	1000	De Pol-Holz et al. (2010)
Brazil Margin	C1 (corals)	22.4°S	40.1°W	621	Mangini et al. (2010)
Brazil Margin	C2 (corals)	24.3°S	43.2°W	781	Mangini et al. (2010)
Drake Passage	Coral	59.7°S	68.7°W	1125	Goldstein et al. (2001)
Drake Passage	Coral	59.4°S	68.5°W	1125	Robinson and van de Flierdt (2009)

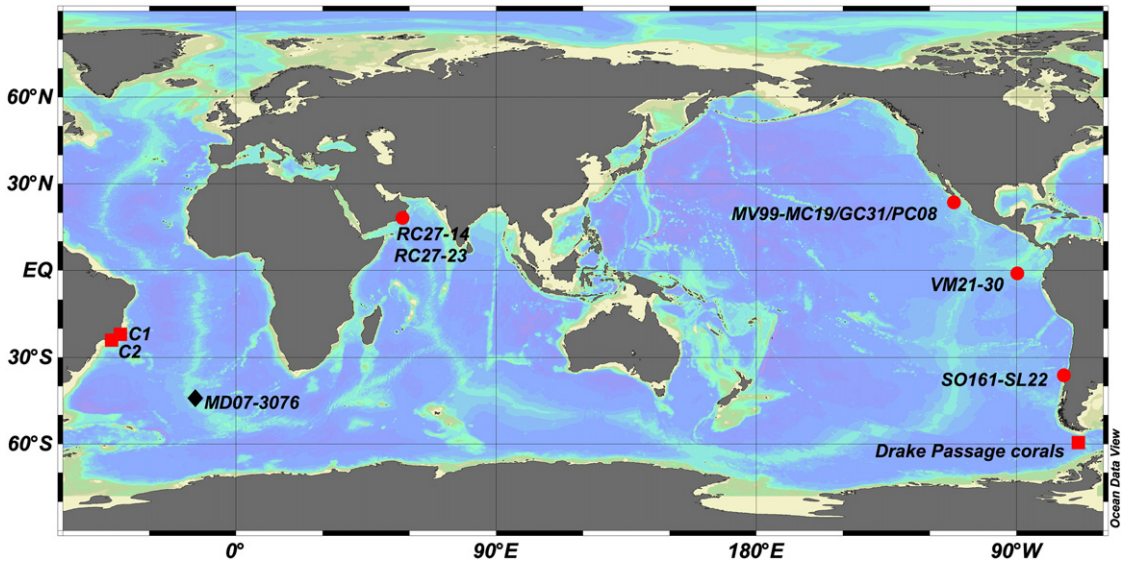

Fig. 1. Location map of sediment core and coral $\Delta^{14}C$ records discussed in this paper. Arabian Sea cores RC27-14 and RC27-23 (this study), Baja California core MV99-MC19/GC31/PC08 (Marchitto et al., 2007), EEP core VM21-30 (Stott et al., 2009), Chile margin core SO161-SL22 (De Pol-Holz et al., 2010), Brazil margin corals C1 and C2 (Mangini et al., 2010) and Drake Passage corals (Goldstein et al., 2001; Robinson and van de Flierdt, 2009) contain records of intermediate water $\Delta^{14}C$ during the last deglaciation. The location of core MD07-3076 (Skinner et al., 2010) in the Atlantic sector of the Southern Ocean is also shown; this core (at 3770 m water depth) records the oldest last glacial maximum deep waters that have been published.

isopycnals with high salinity waters formed from Red Sea and Persian Gulf outflows (You, 1998). However, the volumetric contribution of the outflow waters to the Arabian Sea is small compared to that from intermediate waters entering from the south (Olson et al., 1993; Swallow, 1984), which are composed of Southern Ocean-sourced waters and intermediate waters formed in the Indonesian Seas (Swallow, 1984; Wyrtki, 1973; You, 1998). Lower sea level during the last glacial period would have substantially reduced or eliminated outflow from the marginal seas (Rohling and Zachariasse, 1996), likely increasing the relative proportion of AAIW and SAMW in the Arabian Sea. Stable isotope records from intermediate depths near the Oman margin are consistent with increased southern-sourced waters during glacial periods (Zahn and Pedersen, 1991). Changes in denitrification, aragonite preservation, organic geochemistry, and stable isotopes have also been interpreted to indicate increased presence of oxygen-rich SAMW/AAIW in the Arabian Sea during HS1 and the YD (e.g., Böning and Bard, 2009; Jung et al., 2009; Pichevin et al., 2007; Schulte et al., 1999), consistent with records from the SW Pacific and Atlantic Oceans which suggest enhanced advection of AAIW during these intervals (Pahnke and Zahn, 2005; Pahnke et al., 2008; Rickaby and Elderfield, 2005).

3. Radiocarbon methods

Foraminifera for ^{14}C analysis were picked from the >250 μm sized fraction of previously washed sediment samples. In a few cases benthic foraminifera from the 150–250 μm size fraction were added to increase the sample size. Benthic samples consisted of mixed species of benthic foraminifera. These were mostly infaunal genera including *Globobulimina*, *Bulimina*, *Virgulina*, and *Uvigerina*. Samples did not include any *Pyrgo* spp., which may yield anomalous ^{14}C ages (Nadeau et al., 2001). Planktic samples were monospecifc samples of *G. ruber* or *N. dutertrei*, or mixed *G. ruber* and *G. sacculifer*. Graphite targets were prepared at the INSTAAR Laboratory for AMS Radiocarbon Preparation and Research (NSRL). Foraminifera were leached for 5 min using 0.001 N HCl. Foraminifera were then hydrolyzed using H_3PO_4, and the resultant CO_2 was purified cryogenically. CO_2 was reduced to graphite using an Fe catalyst in the presence of H_2 (McNichol et al., 1992). Oxalic acid primary and secondary measurement standards, geologic control samples of consensus ^{14}C age, and process blanks were prepared along with foraminiferal samples at NSRL. Samples were analyzed for ^{14}C by accelerator mass spectrometry at the Keck Carbon Cycle AMS Facility, UC Irvine (KCCAMS). Results are reported following the conventions of Stuiver and Polach (1977) and corrected for isotopic fractionation using $\delta^{13}C$ measurements of the graphite samples in the AMS. KCCAMS $\delta^{13}C$ values are not suitable for paleoceanographic interpretation, as fractionation can occur during graphitization or AMS measurement, and are not reported here.

4. Results

Radiocarbon ages for RC27-14 and RC27-23 are given in Table 2. We calculated age-corrected $\Delta^{14}C$ values (Fig. 2b) by combining ^{14}C ages with calendar ages derived using the correlation of $\delta^{15}N$ records to GISP2 $\delta^{18}O$ and applying the summary equation for initial $\Delta^{14}C$ of Adkins and Boyle (1997):

$$\Delta^{14}C = (e^{-14C\ age/8033} / e^{-cal\ age/8266} - 1)*1000 \quad (1)$$

where 8033 and 8266 are the Libby and true mean lives of ^{14}C, respectively. Error bars on $\Delta^{14}C$ values were calculated by combining the one-sigma error on the ^{14}C ages with the estimated error in the calendar ages given in Table 2. The $\Delta^{14}C$ errors are dominated by the error in the calendar ages, which causes the error bars to be oriented in a diagonal direction that lies very close to a decay trajectory.

4.1. Evaluation of data quality

One sample depth from RC27-14 and two depths from RC27-23 produced what appear to be anomalous ages (Table 2). $\Delta^{14}C$ values from these samples are either much higher or much lower than the samples immediately above and below in the cores. We are hesitant to interpret large excursions in the $\Delta^{14}C$ data that are not confirmed by either multiple data points or similar patterns between the two cores. Furthermore, results from all three sample depths suggest physically implausible $\Delta^{14}C$ relationships, exhibiting either benthic $\Delta^{14}C$ higher than the atmosphere, planktic $\Delta^{14}C$ much higher than the atmosphere, or planktic $\Delta^{14}C$ lower than benthic $\Delta^{14}C$ in the other core. In the case of the questionable samples from 212 cm (and 222 cm) in RC27-23, the paired planktic and benthic results are both much lower

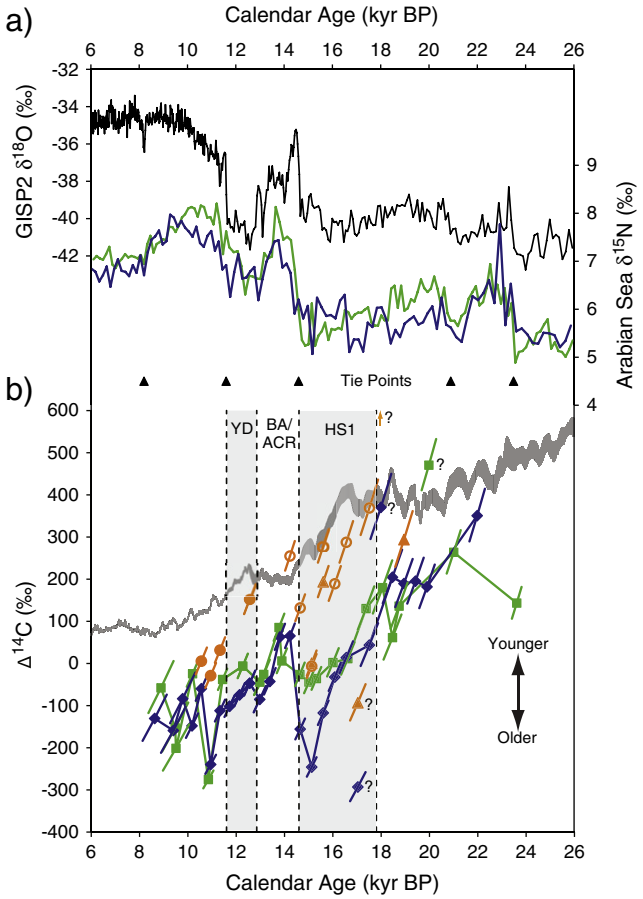

Fig. 2. Arabian Sea sediment core stratigraphy and $\Delta^{14}C$: a) GISP2 $\delta^{18}O$ (Grootes and Stuiver, 1997) and Arabian Sea $\delta^{15}N$ (Altabet et al., 2002) records for the last deglaciation used to construct calendar age models for the sediment cores RC27-14 (shown in green) and RC27-23 (blue). The triangles indicate tie points used to correlate between the sedimentary $\delta^{15}N$ and the GISP2 $\delta^{18}O$ records. b) Arabian Sea intermediate water $\Delta^{14}C$ reconstructed from RC27-14 (green squares) and RC27-23 (blue diamonds); planktonic $\Delta^{14}C$ from RC27-23 (*G. ruber* data are filled orange circles; *G. ruber*/*G. sacculifer* data are open orange circles; and *N. dutertrei* data are orange triangles); and atmospheric $\Delta^{14}C$ (gray line) (Reimer et al., 2009). Error bars on $\Delta^{14}C$ values are based on error on the ^{14}C ages and the determination of calendar ages as described in Section 2. Anomalous $\Delta^{14}C$ values are indicated by question marks. One RC27-23 planktic $\Delta^{14}C$ value from 17,990 yr BP is off of the chart at 905‰. YD, BA, ACR and HS1 indicate the Younger Dryas, Bølling-Allerød, Antarctic Cold Reversal and Heinrich Stadial 1 intervals respectively.

(or higher) than expected, suggesting a process such as lumpy mixing by deep burrowing organisms. If any of the other samples were impacted by deep burrowing, the most likely candidates are 217 cm from RC27-23, the interval in between the two anomalous intervals; and 192 cm in RC27-23, where the planktic $\Delta^{14}C$ is ~290‰ lower than the atmosphere. It should be noted that the exclusion of these two additional intervals would not significantly affect our conclusions. The rest of the data are supported by planktic $\Delta^{14}C$ close to atmospheric values, similar benthic $\Delta^{14}C$ values between the two cores and/or similar benthic $\Delta^{14}C$ values in samples immediately above or below within the core. We have plotted the anomalous values in Figs. 2–4, where they are indicated by question marks, but we do not interpret them as reflective of seawater $\Delta^{14}C$ changes in the following discussion.

The impact of bioturbation of benthic foraminiferal abundance peaks appears to be minimal in RC7-23. Abundances of benthic foraminifera (>150 μm) in RC27-23 were relatively stable during the deglaciation, averaging 310 ± 160 individuals/g (Anderson, 1991) (Fig. 3). Importantly, abundances do not show a trend across the dramatic benthic $\Delta^{14}C$ drop between 227 cm and 192 cm. There is one particularly high count in the benthic abundances at 152 cm, where values reach 870 individuals/g. This abundance peak does not appear to have significantly biased the $\Delta^{14}C$ record. Notably, the benthic ^{14}C age reversal and resulting low $\Delta^{14}C$ value at 142 cm (Table 2) cannot be explained by bioturbation of this abundance peak since the benthic ^{14}C age at 142 cm is ~600 yr older than the benthic age at 152 cm. Abundances of benthic foraminifera were slightly higher during the LGM (440 ± 110 individuals/g) and increased dramatically during the mid-Holocene (reaching a peak of 1110 individuals/g). Since the sedimentation rate in RC27-23 is relatively high (10.5–13.0 cm/kyr) it is unlikely that these abundance changes significantly affected the deglacial $\Delta^{14}C$ record. Benthic foraminiferal abundances were not available in RC27-14.

4.2. Intermediate water $\Delta^{14}C$ history

At ~18 kyr BP, coincident with the start of the atmospheric $\Delta^{14}C$ decline and atmospheric CO_2 rise, intermediate water $\Delta^{14}C$ began to decline at both of the core sites (Fig. 2). $\Delta^{14}C$ at the shallower core site, RC27-14, decreased by ~170‰, reaching a minimum of ~−40‰ at ~15.0 kyr BP. Intermediate water $\Delta^{14}C$ at the RC27-14 core site was as much as ~390‰ lower than the contemporaneous atmosphere at ~16.6 kyr BP. For comparison, in the modern Arabian Sea at ~600 m $\Delta^{14}C$ is only ~100‰ lower than the preindustrial atmosphere (Key et al., 2004). $\Delta^{14}C$ at the deeper Arabian Sea core site, RC27-23, declined by ~440‰ at the beginning of the deglaciation, reaching a minimum of ~−250‰ at ~15.0 kyr BP, ~520‰ lower than the contemporaneous atmosphere. This difference from the atmosphere is much greater than the local preindustrial difference of ~120‰ between the atmosphere and ~800 m and is more than twice as large as the difference between the most ^{14}C-depleted region of the modern ocean (the North Pacific at ~2 km) and the preindustrial atmosphere. This low-$\Delta^{14}C$ interval correlates to Heinrich Stadial 1 (HS1) in the North Atlantic and to early deglacial warming in Antarctica.

During the Bølling–Allerød (B–A) and the synchronous Antarctic Cold Reversal (ACR), intermediate water $\Delta^{14}C$ at both core sites increased, reaching values ~120–140‰ lower than the contemporaneous atmosphere, similar to modern gradients. $\Delta^{14}C$ then declined to values ~220–250‰ lower than the atmosphere in RC27-14 and 260–280‰ lower than the atmosphere in RC27-23 during the Younger Dryas (YD), but in both records this transient ^{14}C depletion appears to continue into the earliest Holocene, when substantially lower $\Delta^{14}C$ values were achieved. We note that the interpretation of the Arabian Sea intermediate water records becomes more complicated near the end of the deglaciation, since outflow from the Red Sea would have resumed as sea level rose. While we remain cautious in interpreting single point excursions, the earliest Holocene negative excursions occur at both core sites with similar timing (i.e., within the estimated error of the age models), and atmospheric $\Delta^{14}C$ does continue to decline until ~9 kyr BP (Reimer et al., 2009). These data may thus reflect the mixing of the last remnants of the isolated glacial deep water mass into the upper ocean.

The planktic $\Delta^{14}C$ from RC27-23 generally falls close to the INTCAL09 atmosphere, with the exception of the intervals corresponding to the largest benthic depletion (HS1) and just following the YD. The lowering of planktic $\Delta^{14}C$ towards benthic values records the local influence of low $\Delta^{14}C$ intermediate waters on the surface ocean. The Arabian Sea cores are located within a strong upwelling zone related to the Southwest Monsoon, and variability within the planktic $\Delta^{14}C$ record can be explained by variability in the strength of upwelling, as well as variability in the $\Delta^{14}C$ of the upwelled water. Following the YD, there is evidence for increased upwelling related to the strengthening of the Southwest Monsoon as indicated by high $\delta^{15}N$ at this time (Altabet et al., 2002), which would increase the subsurface influence on planktic $\Delta^{14}C$ values. Even though the planktic $\Delta^{14}C$ values vary from the

Table 2
Arabian Sea ^{14}C data.

Sample depth (cm)	Calendar age[a] (yr BP)	Calendar age error[b] (yr)	Taxa	Sample weight (mg)	^{14}C age (yr)	^{14}C age error (yr)	$\Delta^{14}C$[c] (‰)	Accession #
RC27-14 (18° 15.2′ N, 57° 39.3′ E, 596 m water depth)								
67	8890	520	Mixed Benthics	4.5	9115	20	−58	CURL-10154
76	9480	540	Mixed Benthics	4.4	10,540	25	−153	CURL-10155
76.5	9510	540	Mixed Benthics	6.5	11,045	25	−201	CURL-9855
87	10,190	240	Mixed Benthics	5.2	10,105	25	−24	CURL-9906
97	10,850	210	Mixed Benthics	6.4	13,130	30	−275	CURL-9918
106	11,440	190	Mixed Benthics	8	11,425	25	−38	CURL-9827
117	12,270	210	Mixed Benthics	7.2	11,975	30	−6	CURL-9916
126	12,980	240	Mixed Benthics	13.8	12,980	25	−44	CURL-9833
128	13,140	250	Mixed Benthics	4.9	12,980	40	−26	CURL-10156
136	13,770	220	Mixed Benthics	7.6	12,725	25	85	CURL-10159
137.5	13,890	210	Mixed Benthics	11.5	13,450	30	6	CURL-9837
147	14,630	200	Mixed Benthics	4.4	14,435	35	−26	CURL-9910
152.5	15,010	200	Mixed Benthics	10.3	14,950	30	−44	CURL-9842
157	15,320	200	Mixed Benthics	6.3	15,180	30	−36	CURL-9923
167	16,000	240	Mixed Benthics	9.5	15,535	35	2	CURL-9907
176	16,620	280	Mixed Benthics	11.5	16,060	35	11	CURL-9843
187	17,370	340	Mixed Benthics	5.5	15,900	35	130	CURL-9915
197	18,060	400	Mixed Benthics	7.1	16,220	40	180	CURL-9914
203	18,470	370	Mixed Benthics	6	17,470	45	61	CURL-9830
207	18,740	350	Mixed Benthics	6.3	17,190	45	136	CURL-9920
225[d]	19,980	300	Mixed Benthics	8.4	16,315	40	470	CURL-9828
240	21,000	290	Mixed Benthics	7.8	18,530	45	264	CURL-9836
275	23,610	200	Mixed Benthics	7.9	21,870	70	143	CURL-9852
RC27-23 (17° 59.6′ N, 57° 35.4′ E, 820 m water depth)								
112	8630	500	Mixed Benthics	5.6	9505	20	−130	CURL-10999
122	9400	510	Mixed Benthics	3.5	10,525	25	−159	CURL-10991
127	9780	520	Mixed Benthics	6.1	10,210	20	−84	CURL-10488
132	10,170	250	Mixed Benthics	3.1	11,170	30	−148	CURL-10993
137	10,560	230	*G. ruber*	3.9	10,215	30	−6	CURL-11156
137	10,560	230	Mixed Benthics	6.3	10,755	25	−60	CURL-10484
142	10,940	220	*G. ruber*	4.2	10,870	30	−29	CURL-11157
142	10,940	220	Mixed Benthics	8	12,835	25	−240	CURL-10466
147	11,330	210	*G. ruber*	4.1	10,760	30	32	CURL-11158
147	11,330	210	Mixed Benthics	5.6	11,965	30	−112	CURL-10469
152	11,730	210	Mixed Benthics	10.1	12,255	25	−102	CURL-10487
157	12,140	220	Mixed Benthics	6	12,420	25	−74	CURL-10468
162	12,560	230	*G. ruber*	4.1	11,065	25	152	CURL-11151
162	12,560	230	Mixed Benthics	8.1	12,590	25	−47	CURL-9829
167	12,980	250	Mixed Benthics	8.5	13,325	30	−85	CURL-10465
172	13,390	240	Mixed Benthics	7.1	13,365	30	−43	CURL-10470
177	13,810	210	Mixed Benthics	10.2	12,930	30	63	CURL-10486
182	14,230	200	*G. ruber/G. sacculifer*	5.8	12,000	30	255	CURL-11137
182	14,230	200	Mixed Benthics	11.1	13,315	25	65	CURL-10483
187	14,650	200	*G. ruber/G. sacculifer*	4.9	13,240	30	132	CURL-11145
187	14,650	200	Mixed Benthics	3.2	15,595	40	−156	CURL-10464
192	15,130	200	*G. ruber/G. sacculifer*	4.2	14,750	35	−6	CURL-11148
192	15,130	200	*N. dutertrei*	3	14,695	45	0	CURL-10989
192	15,130	200	Mixed Benthics	5.7	16,965	50	−246	CURL-10160
197	15,600	220	*G. ruber/G. sacculifer*	4.9	13,190	35	278	CURL-11155
197	15,600	220	*N. dutertrei*	3.5	13,740	35	194	CURL-10992
197	15,600	220	Mixed Benthics	8.8	16,165	50	−117	CURL-10157
202	16,080	250	*G. ruber/G. sacculifer*	3.8	14,235	35	189	CURL-11146
202	16,080	250	Mixed Benthics	8.3	15,890	35	−32	CURL-10153
207	16,560	280	*G. ruber/G. sacculifer*	4.1	14,060	35	288	CURL-11154
207	16,560	280	Mixed Benthics	7.7	15,980	30	14	CURL-10481
212[d]	17,030	320	*N. dutertrei*	2.3	17,340	70	−93	CURL-10983
212[d]	17,030	320	Mixed Benthics	9.3	19,340	80	−293	CURL-10161
217	17,510	360	*G. ruber/G. sacculifer*	3.6	14,495	35	369	CURL-11147
217	17,510	360	Mixed Benthics	7.2	16,675	40	44	CURL-10474
222[d]	17,990	430	*N. dutertrei*	3.8	12,305	30	905	CURL-10996
222[d]	17,990	430	Mixed Benthics	7.4	14,950	35	370	CURL-10162
227	18,470	400	Mixed Benthics	6.3	16,450	35	205	CURL-10490
232	18,940	360	*N. dutertrei*	3.1	16,340	60	294	CURL-10982
232	18,940	360	Mixed Benthics	5.4	17,015	35	190	CURL-10463
237	19,420	340	Mixed Benthics	5.5	17,440	35	195	CURL-10477
242	19,900	320	Mixed Benthics	7.9	17,995	40	182	CURL-10480
262	21,970	320	Mixed Benthics	6.5	18,940	60	351	CURL-9850

[a] Calendar ages derived from correlation between sediment $\delta^{15}N$ and GISP2 $\delta^{18}O$ as described in Section 2.
[b] Calendar age errors based on the precision of tie points and uncertainty in sedimentation rates as described in Section 2.
[c] $\Delta^{14}C$ calculated from ^{14}C ages and calendar ages using Equation 1.
[d] These intervals yielded anomalously young or old ^{14}C ages.

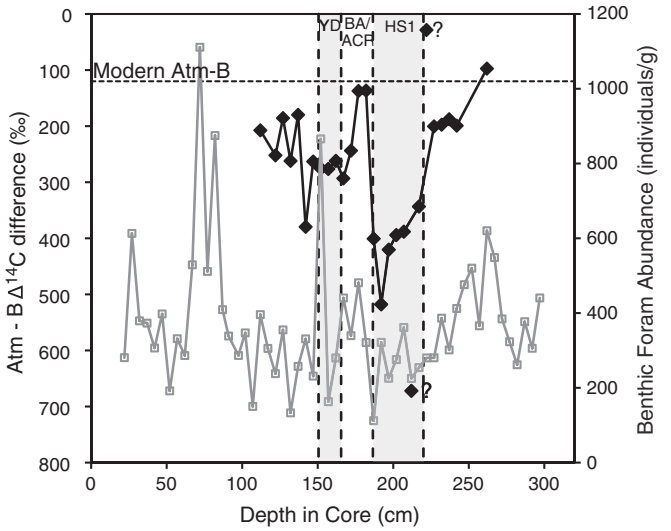

Fig. 3. Comparison of RC27-23 benthic foraminiferal abundances and intermediate water ^{14}C depletions. Benthic foraminifera abundance data shown in gray open squares are from Anderson (1991). Atmosphere — benthic $\Delta^{14}C$ differences are shown in black filled diamonds. Atmospheric values are average Intcal09 (Reimer et al., 2009) values for the time interval surrounding each calendar age ± the calendar age errors. The modern Atmosphere — benthic $\Delta^{14}C$ difference for ~800 m in the Arabian Sea is indicated by a dashed line. Benthic $\Delta^{14}C$ values determined to be anomalous (see Section 4.1) are indicated by question marks. YD, BA, ACR and HS1 indicate the Younger Dryas, Bølling-Allerød, Antarctic Cold Reversal and Heinrich Stadial 1 intervals respectively.

expected warm surface ocean values at times, the reduction in benthic $\Delta^{14}C$ at RC27-23 during the HS1 interval is confirmed by very large benthic–planktic age differences, ranging from 1.7 to 3.0 kyr. We also note that the greater magnitude of the intermediate water $\Delta^{14}C$ decline, compared to the atmospheric and planktic $\Delta^{14}C$ decreases, indicates that the ^{14}C-depleted carbon observed during HS1 was sourced from the ocean, rather than reflecting equilibration with an atmospheric $\Delta^{14}C$ change. Additionally, the smaller $\Delta^{14}C$ decline recorded in RC27-14 during HS1, relative to RC27-23, indicates that the core of the low-$\Delta^{14}C$ water lay below the depth of RC27-14. The $\Delta^{14}C$ values recorded by RC27-14 during HS1 reflect the mixing between low-$\Delta^{14}C$ waters below and higher-$\Delta^{14}C$ waters above.

5. Discussion

^{14}C-depleted intermediate waters during the deglaciation have been previously recorded at two sites in the eastern Pacific (Marchitto et al., 2007; Stott et al., 2009) (Table 1; Fig. 1). Intermediate water $\Delta^{14}C$ reconstructed for the Arabian Sea during the deglaciation is similar to that reconstructed for the eastern North Pacific near Baja California (Marchitto et al., 2007) (Fig. 4). In particular, the timing and magnitude of ^{14}C depletion recorded in the deeper Arabian Sea core during the HS1 interval is almost identical to that of the Baja record, and the Arabian Sea and Baja California records rebound to similar values during the B–A. However, the appearance of the YD ^{14}C-depletion in the Arabian Sea is significantly different from that observed near Baja California. The Arabian Sea records do not reach values as low as those near Baja California, and while the Baja California record reaches a local minimum during the YD, the Arabian Sea records continue to decline, reaching minima after the YD. The $\Delta^{14}C$ record from the EEP (Stott et al., 2009) exhibits a broad minimum without the millennial-scale features evident in the Arabian Sea and Baja California records. The $\Delta^{14}C$ values in the EEP are also extremely low, with values reaching ~800‰ lower than the atmosphere at times. These features suggest that the source of the low $\Delta^{14}C$ values or the processes involved in transporting ^{14}C-depeted water to the EEP site were different than those responsible for the Arabian Sea and Baja California records. While it is possible that the low $\Delta^{14}C$ values recorded at Baja California could be explained by episodic transport of low $\Delta^{14}C$ waters from a proximate source in the EEP, it is very unlikely that this can explain the similar findings in the Arabian Sea.

The strong similarity between the deeper Arabian Sea record and the Baja California record during HS1 and the B–A suggests that similar mechanisms were involved in controlling the $\Delta^{14}C$ at these two sites. The similar response at these distant sites also indicates that the cause of ^{14}C depletion is likely oceanographic in origin, rather than locally sourced ^{14}C-dead geologic CO_2. In the following discussion we evaluate three different mechanisms that may have played a role in controlling the $\Delta^{14}C$ of intermediate waters in the Arabian Sea and near Baja California: *in situ* aging of intermediate waters, local upwelling of low-^{14}C carbon from the deep ocean, and advection of low-^{14}C carbon to the sites via intermediate waters. We focus here on the $\Delta^{14}C$ decline during the HS1 interval, since it is well defined at both sites and corresponds to the largest changes in atmospheric $\Delta^{14}C$ and pCO_2. While the same arguments can generally be applied to the YD interval, other processes such as differential water mass mixing or local upwelling likely led the Arabian Sea and Baja California to diverge during the YD.

An important constraint on the mechanisms involved in the $\Delta^{14}C$ declines in the Arabian Sea and near Baja California is the apparent decoupling between $\Delta^{14}C$ and $[O_2]$ during HS1 and the YD. As was discussed above, the modern Arabian Sea contains a large oxygen minimum zone and undergoes significant denitrification. The $\delta^{15}N$ records from RC27-14 and RC27-23 (Altabet et al., 2002) and other sites in the Arabian Sea (e.g., Pichevin et al., 2007) indicate reduced denitrification (and hence higher oxygen concentrations) during HS1 and the YD. Reduced organic carbon and sedimentary Mo concentrations in the Baja California core also indicate higher intermediate

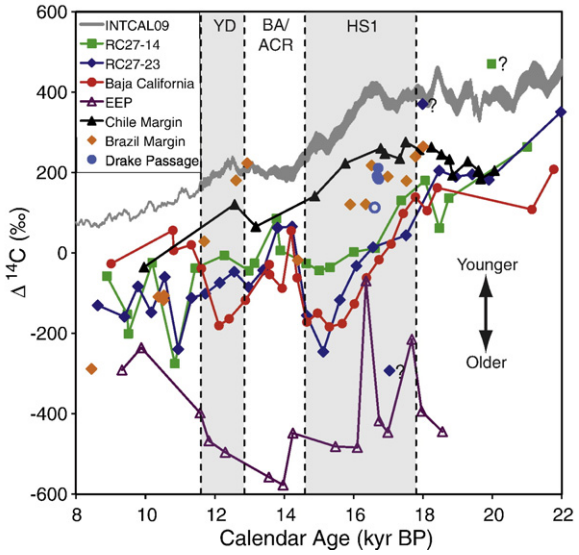

Fig. 4. Comparison of the deglacial intermediate water $\Delta^{14}C$ data: Arabian Sea records, shown in green squares (RC27-14) and dark blue diamonds (RC27-23), Baja California (red circles) (Marchitto et al., 2007), Eastern Equatorial Pacific (EEP) (purple open triangles) (Stott et al., 2009), Chile Margin (black triangles) (De Pol-Holz et al., 2010), Brazil Margin corals (orange diamonds) (Mangini et al., 2010), and the Drake Passage corals (Robinson and van de Flierdt, 2009—closed light blue circles; and Goldstein et al., 2001—open light blue circle). The INTCAL09 atmospheric $\Delta^{14}C$ record (Reimer et al., 2009) is also shown in gray. De Pol-Holz et al. (2010) used calibrated planktonic foraminiferal ^{14}C ages for calendar ages; these ^{14}C ages have been recalibrated here using MARINE09 (Reimer et al., 2009) (400 yr reservoir age) to allow direct comparison with the INTCAL09 atmosphere. YD, BA, ACR and HS1 indicate the Younger Dryas, Bølling-Allerød, Antarctic Cold Reversal and Heinrich Stadial 1 intervals respectively.

water oxygen concentrations during these intervals (Dean et al., 2006; Ortiz et al., 2004). Higher oxygen concentrations during intervals of lower $\Delta^{14}C$ are somewhat counterintuitive. In general, $\Delta^{14}C$ and $[O_2]$ are well correlated in the ocean, with low $\Delta^{14}C$ values corresponding to low $[O_2]$. Both ^{14}C and O_2 are renewed in the surface ocean through gas exchange with the atmosphere. The longer a water mass resides within the ocean interior, the more ^{14}C is lost to decay and the more O_2 is consumed by the oxidation of organic matter. We would expect that an isolated deep water mass that is depleted in ^{14}C would also have very low $[O_2]$. However, $\Delta^{14}C$ and $[O_2]$ can become decoupled during the process of air–sea gas exchange. This is due to the large difference in the timescale of air–sea oxygen exchange compared to that for isotopic equilibration of CO_2 (a month vs. a decade, respectively, for a mixed layer depth of 80 m) (Broecker and Peng, 1974). Thus, decoupling can occur for water-parcels with residence times at or near the surface that are close to the timescale for gas exchange, but significantly less than for carbon isotopic exchange. In the modern ocean this process occurs to varying degrees in the modern Southern Ocean in the formation region of AAIW, where $[O_2]$ is renewed to saturation but $\Delta^{14}C$ is not fully equilibrated with the atmosphere (Key et al., 2004). This oxygen constraint plays a prominent role in our assessment of the possible mechanisms described below.

5.1. In situ aging of intermediate waters

The rate of decline in intermediate water $\Delta^{14}C$ that occurs near Baja California and in the Arabian Sea at the start of the deglaciation is similar to or slightly greater than the rate of ^{14}C decay. Both the Baja California and Arabian Sea sites are located in regions that are outside of direct thermocline ventilation (cf. Luyten et al., 1983). How much of the ^{14}C depletion may be explained simply by isolation and localized aging of the intermediate water at these sites? In the absence of lateral advection along isopycnals, the ventilation timescale will be set by the rate of turbulent diffusive mixing. Vertical diffusive mixing across the thermocline is relatively slow, given the strong density gradient. If we assume a typical vertical diffusion coefficient for the thermocline of 10^{-5} m^2/s, and a depth of 700 m for RC27-23 (incorporating a glacial reduction of sea level of 120 m (Fairbanks, 1989)) we can estimate a timescale for mixing of ~1500 yr. If vertical diffusion was the only mechanism of ^{14}C renewal, then aging may have explained a significant proportion of the $\Delta^{14}C$ decline. However, these sites are not horizontally isolated from the rest of the ocean basin and rates of mixing along isopycnals are much more rapid than vertical mixing. For example, assuming a typical basin scale horizontal diffusion coefficient of 1000 m^2/s, and a length scale of 1000 km, the mixing timescale is on the order of decades. A decadal timescale is consistent with CFC estimates of the ventilation age of modern Arabian Sea intermediate waters (Fine et al., 2008). In order to explain a significant portion of the $\Delta^{14}C$ decline, the horizontal diffusion coefficient would need to be about 2 orders of magnitude smaller.

An *in situ* aging mechanism would also violate the oxygen constraint. Oxygen concentrations reflect the balance between oxygen supply and oxidant demand due to the remineralization of exported carbon from primary production. While there is some disagreement as to which factor dominates in the Arabian Sea and off Baja California, in order to explain both the isolation of waters for centuries to thousands of years and higher than modern oxygen concentrations, productivity would have to be essentially shut off. Reconstructions do indicate reduced productivity in the Arabian Sea (Altabet et al., 2002; Pourmand et al., 2007) and off Baja California (Ortiz et al., 2004) during HS1. However, productivity was not eliminated entirely, and without the renewal of oxygen from advection of intermediate and thermocline waters or horizontal diffusive mixing, O_2 concentrations should have been depleted rapidly. We therefore reject *in situ* aging of intermediate waters as a significant contributor to the HS1 $\Delta^{14}C$ decline.

5.2. Local upward mixing of ^{14}C-depleted carbon

Another possible mechanism that may have contributed to the $\Delta^{14}C$ decline is local upward mixing of ^{14}C-depleted carbon from the deep ocean. Since the deep ^{14}C-depleted waters would have to mix extensively with overlying, less ^{14}C-depleted waters, the signal would be substantially diluted by the time it reached our core sites, requiring the deep waters to be much more depleted than the largest depletion seen in our intermediate water cores. The absolute amount of depletion required will be dependent on the volume occupied by the deep water mass and the amount of mixing that occurred. Since the hypothetical ^{14}C-depleted deep ocean reservoir appears to be limited to deeper than ~3 km (Broecker et al., 2007), this deep water mass would have to be extremely old. This scenario also requires that the upward mixing of deep waters in the Indian and Pacific Oceans responded rapidly to a common trigger, increasing at the beginning of the deglaciation and shutting off at the start of the Bølling. The similarity between the Arabian Sea and Baja California records further requires that the deep water $\Delta^{14}C$ and the amount of mixing with overlying waters be very similar between the northern Indian Ocean and the eastern North Pacific.

Local upward mixing of deep waters would also likely violate the local oxygen constraint. Extremely old deep waters would be expected to have very low oxygen concentrations (cf. Jaccard et al., 2009). These initially very low oxygen levels would be rapidly consumed by respiration in the intermediate depth ocean. While we cannot rule out some contribution of locally upwelled, low-$\Delta^{14}C$ deep water to intermediate waters of the Arabian Sea and those off Baja California, this mechanism seems unlikely to be the primary control on intermediate water $\Delta^{14}C$.

5.3. Advection of ^{14}C-depleted carbon via intermediate waters

The third possible mechanism that may explain the HS1 $\Delta^{14}C$ decline is the incorporation of ^{14}C-depleted deep sea carbon into an intermediate water mass and advection of that water to the Arabian Sea and Baja California core sites. Indeed, the easiest way to explain the strong similarity between the Arabian Sea and Baja California records is to invoke ventilation by a common water mass. The incorporation and transport of the aged carbon by such an intermediate water mass would also relieve the oxygen constraint. The relatively brief timescale required for conversion of upwelled deep waters to intermediate water by the addition of buoyancy may permit oxygen to be renewed without significantly influencing $\Delta^{14}C$. We also note that if the greater aragonite preservation observed by Böning and Bard (2009) in the Arabian Sea during HS1 is primarily a result of higher preformed intermediate water $[CO_3^{2-}]$, then the upwelled deep waters must have also released much of their excess CO_2 to the atmosphere during the conversion to intermediate waters. However, carbonate preservation may also be affected by changes in pore-water dissolution related to variability in organic carbon flux to the sediments (Emerson and Bender, 1981).

If we conclude that the advection of ^{14}C-depleted carbon to the Arabian Sea and Baja California via an intermediate water mass is the most likely explanation, the next question is where were the intermediate waters formed. A Southern Ocean source is supported by several observations: 1) the main connection between the Indian Ocean and the Pacific Ocean is through the Southern Ocean. In the modern ocean, well-oxygenated AAIW flows into each of the major ocean basins, ventilating the intermediate waters throughout the Southern Hemisphere and Northern Tropics (Sloyan and Rintoul, 2001; Talley, 1999). 2) The Southern Ocean is the only location in the modern ocean where carbon and nutrient rich deep waters upwell to

the surface. The direct incorporation of old deep water into intermediate waters with limited mixing would minimize the required age of the glacial ^{14}C-depleted deep water. 3) As we have already noted, the formation region of AAIW/SAMW in the Southern Ocean is the only region in the modern ocean where processes of deep-to-intermediate water mass conversion permit decoupling of performed [O_2] and Δ^{14}C. 4) The timing of the intermediate water Δ^{14}C depletions is coincident with warming in Antarctica (Monnin et al., 2001) and increased upwelling in the Southern Ocean (Anderson et al., 2009), providing a mechanism for the return of old deep waters to the upper ocean (Fig. 5). The increasing depletion of ^{14}C during HS1 observed in the Arabian Sea and near Baja California is likely related to a combination of increasing deep upwelling in the Southern Ocean, which tapped progressively into deeper, more depleted waters, and the continued aging of the densest deep waters. 5) Modeling studies have shown a see-saw type behavior in the NADW and AAIW overturning circulations (Keeling and Stephens, 2001; Saenko et al., 2003; Schulte et al., 1999; Sijp and England, 2006), in which a decrease in the NADW production, as occurred during HS1 and the YD (McManus et al., 2004), leads to an enhancement of AAIW production. These results are consistent with paleoceanographic observations that indicate increased advection of AAIW during HS1 and the YD (e.g., Bostock et al., 2004; Pahnke and Zahn, 2005; Pahnke et al., 2008; Rickaby and Elderfield, 2005), as well as a tight coupling between NADW and AAIW formation for the past 340 kyr (Pahnke and Zahn, 2005).

The input of nutrient and carbon rich waters into SAMW and AAIW is consistent with the widespread minima in δ^{13}C recorded in planktonic foraminifera and intermediate depth benthic foraminifera from the southern hemisphere and northern tropics during deglaciations (e.g., Curry and Crowley, 1987; Ninnemann and Charles, 1997; Oppo and Fairbanks, 1987; Spero and Lea, 2002), as well as the deglacial increases in productivity and oxidant demand in the Eastern Equatorial Pacific (e.g., Loubere and Bennett, 2008; Martinez and Robinson, 2010; Robinson et al., 2009). Unfortunately the infaunal benthic foraminifera that dominate the assemblages in the Arabian Sea and Baja California cores do not allow us to assess the preformed δ^{13}C signal that should be associated with the low Δ^{14}C values.

A challenge to Southern Ocean upwelling of ^{14}C-depleted carbon is the lack of a Δ^{14}C decline in the intermediate waters along the Chile margin (De Pol-Holz et al., 2010). This site is ventilated by AAIW in the modern ocean, and if ^{14}C-depleted waters were upwelled in the Southern Ocean we would expect to see low Δ^{14}C values at this site. Yet there is no evidence for the influx of ^{14}C-depleted waters during the deglaciation at this site. In fact, intermediate water Δ^{14}C values recorded at this site *increase* during the deglaciation and follow the atmosphere closely (Fig. 4), which is unexpected for waters sourced in the Southern Ocean, especially at a time of increased Southern Ocean upwelling (Anderson et al., 2009). The waters that bathed the Chile margin must have spent enough time at the surface to become isotopically well equilibrated with the atmosphere.

It is possible that a Southern Ocean source of low-Δ^{14}C intermediate waters may be reconciled with the lack of ^{14}C depletion along the Chile margin if there were multiple regions of AAIW formation in the deglacial Southern Ocean. The intermediate waters that bathed the Chile margin likely formed in the southeast Pacific, just west of the Drake Passage, where the majority of modern AAIW forms today (McCartney, 1977; Talley, 1996). Corals from intermediate waters in the Drake Passage record only a small decrease in Δ^{14}C during HS1 relative to modern gradients (Goldstein et al., 2001; Robinson and van de Flierdt, 2009) (Fig. 4), consistent with the formation of relatively well-ventilated intermediate waters in the southeast Pacific. Coral records from intermediate waters along the Brazil margin also agree well with those from the Drake Passage during HS1 (Mangini et al., 2010), suggesting that the Brazil margin waters were also formed in the southeast Pacific. Thus, the available records appear to limit the regions of deep-to-intermediate water mass conversion under conditions of poor carbon isotopic equilibration to the Atlantic, Indian and southwest Pacific sectors of the Southern Ocean. Today, much of the ^{14}C depletion signal carried to the areas of upwelling in the EEP originates in the southwest Pacific sector, off of Tasmania (Toggweiler et al., 1991). This is compatible with an influence of the southwest Pacific sector on the Baja Margin, while an influence of the Atlantic and Indian Ocean sectors on the Arabian Sea sites is also to be expected. Additional records from or downstream of these areas will be needed in order to test this hypothesis.

A less likely possibility is that the low-Δ^{14}C waters at both the Baja Margin and in the Arabian Sea were sourced from the North Pacific. The reconstructed increase in North Pacific Deep Water (NPDW) ventilation during the deglaciation suggests that the North Pacific may have been a source of at least some ^{14}C-depleted carbon to the upper ocean and atmosphere during deglaciation (e.g., Galbraith et al., 2007; Okazaki et al., 2010), although the reconstructed NPDW Δ^{14}C values are not low enough to explain the Arabian Sea or Baja California results. If low-Δ^{14}C deep waters did upwell to the surface of the North Pacific, O_2 could have been renewed during the conversion to North Pacific Intermediate Water (NPIW) in a process analogous to the

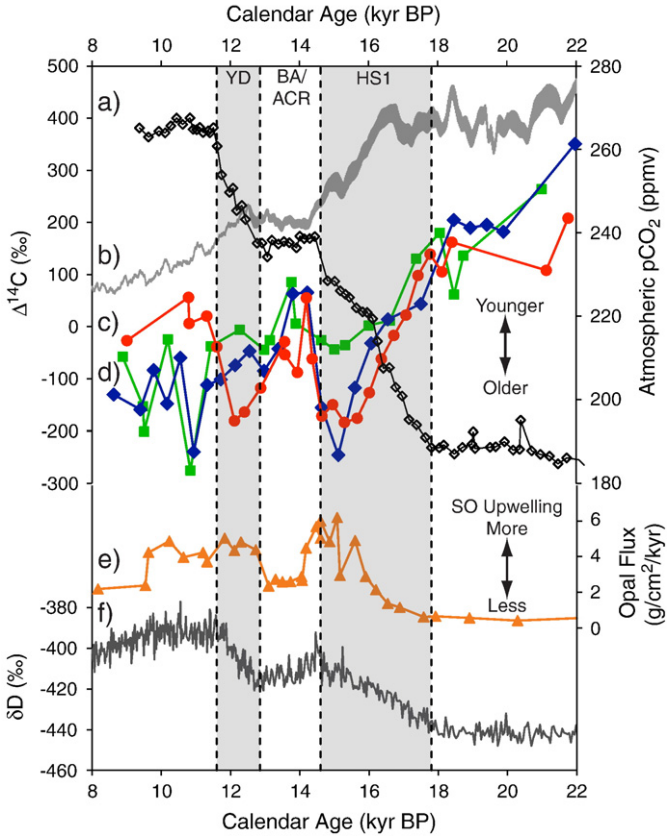

Fig. 5. Compilation of carbon cycle and climate changes during the last deglaciation: a) Atmospheric CO_2 concentration measured in the Dome C ice core (black open diamonds) (Monnin et al., 2001), placed on the GISP2 timescale using methane synchronization (Marchitto et al., 2007). b) INTCAL09 atmospheric Δ^{14}C record (gray line) (Reimer et al., 2009). c) Baja California intermediate water Δ^{14}C (red circles) (Marchitto et al., 2007). d) Arabian Sea intermediate water Δ^{14}C from RC27-14 (green squares) and RC27-23 (blue diamonds). e) Southern Ocean opal flux (orange triangles) indicating the strength of Southern Ocean (SO) upwelling (Anderson et al., 2009). f) Antarctic Dome C δD (gray line) (Jouzel et al., 2007) placed on the GISP2 timescale (Marchitto et al., 2007). YD, BA, ACR and HS1 indicate the Younger Dryas, Bølling-Allerød, Antarctic Cold Reversal and Heinrich Stadial 1 intervals respectively.

modern deep-intermediate water conversion in the Southern Ocean. This hypothetical deglacial version of NPIW would likely need to form farther east than modern NPIW, since benthic–planktic ^{14}C pairs from cores in the northwest Pacific indicate young, ^{14}C-equilibrated intermediate waters during the deglaciation (e.g., Ahagon et al., 2003; Duplessy et al., 1989; Okazaki et al., 2010). While the incorporation of low-$\Delta^{14}C$ waters into NPIW may have influenced Baja California record, it is difficult to explain the Arabian Sea results in this manner. The North Pacific signal would need to reach the Arabian Sea via the Indonesian Throughflow (ITF). In the modern ITF, the lower thermocline and intermediate waters are sourced from the South Pacific, and the ITF waters undergo intense mixing as they cross the various sills in the Indonesian Seas (e.g., Gordon and Fine, 1996; Gordon et al., 2003; Talley and Sprintall, 2005). These features make it unlikely that a North Pacific signal could reach the Arabian Sea without significant dilution. Lower sea level would have also reduced the maximum sill depths within the Indonesian Seas, restricting the passage of the densest through-flow waters.

6. Conclusions

In this study we have reconstructed the $\Delta^{14}C$ at intermediate depths in the Arabian Sea during the last deglaciation. These reconstructions reveal intermediate waters that were very depleted in ^{14}C relative to the contemporaneous atmosphere, with the deeper core site recording lower $\Delta^{14}C$ values than the shallower site. The timing of the low $\Delta^{14}C$ intervals is coincident with increases in atmospheric pCO_2 and decreases in atmospheric $\Delta^{14}C$. The $\Delta^{14}C$ reconstructed for the Arabian Sea is similar to that previously recorded in the eastern North Pacific near Baja California, particularly during Heinrich Stadial 1. The similarity in the $\Delta^{14}C$ records between these two distant sites suggests that similar mechanisms were responsible for the observations and that the processes involved are likely oceanographic in origin rather than geologic.

The intermediate water $\Delta^{14}C$ records in the Arabian Sea and near Baja California are most readily consistent with the upwelling of ^{14}C-depleted deep water up to the surface of the Southern Ocean as this ocean warmed and destratified during the deglaciation. These ^{14}C-depleted waters must have spent enough time near the surface of the Southern Ocean to gain buoyancy and renew oxygen concentrations, but not enough time to significantly alter $\Delta^{14}C$, before being incorporated into thermocline or intermediate waters such as Subantarctic Mode Water or Antarctic Intermediate Water.

At this time, significant outstanding questions remain. It is unclear why ^{14}C-depleted waters are not observed along the Chile margin (De Pol-Holz et al., 2010). It is also unclear how the $\Delta^{14}C$ record from the intermediate Eastern Equatorial Pacific (Stott et al., 2009) is related to the records from the Arabian Sea or Baja California. The difference in timing and structure as well as the much lower $\Delta^{14}C$ values suggests that the mechanisms involved in transporting ^{14}C-depleted carbon to the EEP site were different. The spatial and temporal coverage of $\Delta^{14}C$ records from the glacial and deglacial ocean remains very sparse. Effort should be made to reconstruct intermediate water $\Delta^{14}C$ from other sites, especially from the southern high latitudes. Mapping of the glacial ^{14}C-depleted deep reservoir also remains a major priority.

Acknowledgements

We are grateful to David Anderson for providing sediment samples and for numerous discussions, Warren Prell for providing sediment samples; Chad Wolak and Patrick Cappa for laboratory assistance; and John Southon for accelerator mass spectrometry analyses. We thank Ricardo de Pol-Holz and three anonymous reviewers for their constructive and thorough reviews, which improved this manuscript. This work was funded by National Science Foundation grant OCE-0851391 to SJL and TMM, an ExxonMobil Geoscience Grant to SPB and a CU Geological Sciences/Shell Research Grant to SPB.

References

Adkins, J.F., Boyle, E.A., 1997. Changing atmospheric Delta C-14 and the record of deep water paleoventilation ages. Paleoceanography 12 (3), 337–344.
Adkins, J.F., McIntyre, K., Schrag, D.P., 2002. The salinity, temperature, and delta O-18 of the glacial deep ocean. Science 298 (5599), 1769–1773.
Ahagon, N., Ohkushi, K., Uchida, M., Mishima, T., 2003. Mid-depth circulation in the northwest Pacific during the last deglaciation: evidence from foraminiferal radiocarbon ages. Geophys. Res. Lett. 30 (21). doi:10.1029/2003gl018287.
Altabet, M.A., Higginson, M.J., Murray, D.W., 2002. The effect of millennial-scale changes in Arabian Sea denitrification on atmospheric CO2. Nature 415 (6868), 159–162.
Anderson, D.M., 1991. Foraminifer Evidence of Monsoon Upwelling off Oman During the Late Quaternary. Brown University, Providence, RI.
Anderson, R.F., et al., 2009. Wind-driven upwelling in the Southern Ocean and the deglacial rise in atmospheric CO2. Science 323 (5920), 1443–1448.
Archer, D., Winguth, A., Lea, D., Mahowald, N., 2000. What caused the glacial/interglacial atmospheric pCO(2) cycles? Rev. Geophys. 38 (2), 159–189.
Barker, S., Broecker, W.S., Clark, E., Hajdas, I., 2007. Radiocarbon age offsets of foraminifera resulting from differential dissolution and fragmentation within the sedimentary bioturbated zone. Paleoceanography 22 (2), PA2205. doi:10.1029/2006pa001354.
Böning, P., Bard, E., 2009. Millennial/centennial-scale thermocline ventilation changes in the Indian Ocean as reflected by aragonite preservation and geochemical variations in Arabian Sea sediments. Geochim. Cosmochim. Acta 73 (22), 6771–6788.
Bostock, H.C., Opdyke, B.N., Gagan, M.K., Fifield, L.K., 2004. Carbon isotope evidence for changes in Antarctic Intermediate Water circulation and ocean ventilation in the southwest Pacific during the last deglaciation. Paleoceanography 19 (4).
Brandes, J.A., Devol, A.H., Yoshinari, T., Jayakumar, D.A., Naqvi, S.W.A., 1998. Isotopic composition of nitrate in the central Arabian Sea and eastern tropical North Pacific: a tracer for mixing and nitrogen cycles. Limnol. Oceanogr. 43 (7), 1680–1689.
Broecker, W.S., 1982. Glacial to interglacial changes in ocean chemistry. Prog. Oceanogr. 11 (2), 151–197.
Broecker, W.S., Barker, S., 2007. A 190% drop in atmosphere's Delta(14)C during the "Mystery Interval" (17.5 to 14.5 kyr). Earth Planet. Sci. Lett. 256 (1–2), 90–99.
Broecker, W.S., Peng, T.H., 1974. Gas-exchange rates between air and sea. Tellus 26 (1–2), 21–35.
Broecker, W., et al., 2004a. Ventilation of the glacial deep Pacific Ocean. Science 306 (5699), 1169–1172.
Broecker, W.S., Clark, E., Hajdas, I., Bonani, G., 2004b. Glacial ventilation rates for the deep Pacific Ocean. Paleoceanography 19 (2), PA2002. doi:10.1029/2003pa000974.
Broecker, W.S., et al., 2007. Radiocarbon age of late glacial deep water from the equatorial Pacific. Paleoceanography 22 (2), Pa2206. doi:10.1029/2006pa001359.
Broecker, W., Clark, E., Barker, S., 2008. Near constancy of the Pacific Ocean surface to mid-depth radiocarbon-age difference over the last 20 kyr. Earth Planet. Sci. Lett. 274 (3–4), 322–326.
Burns, S.J., Fleitmann, D., Matter, A., Kramers, J., Al-Subbary, A.A., 2003. Indian Ocean climate and an absolute chronology over Dansgaard/Oeschger events 9 to 13. Science 301 (5638), 1365–1367.
Cline, J.D., Kaplan, I.R., 1975. Isotopic fractionation of dissolved nitrate during denitrification in the eastern tropical north Pacific Ocean. Mar. Chem. 3, 271–299.
Curry, W.B., Crowley, T.J., 1987. The $\delta^{13}C$ of Equatorial Atlantic surface waters: implications for ice age pCO_2 levels. Paleoceanography 2 (5), 489–517.
Curry, W.B., Oppo, D.W., 2005. Glacial water mass geometry and the distribution of delta C-13 of Sigma CO2 in the western Atlantic Ocean. Paleoceanography 20 (1), Pa1017. doi:10.1029/2004pa001021.
De Pol-Holz, R., Keigwin, L., Southon, J., Hebbeln, D., Mohtadi, M., 2010. No signature of abyssal carbon in intermediate waters off Chile during deglaciation. Nat. Geosci. 3, 192–195.
Dean, W.E., Zheng, Y., Ortiz, J.D., van Geen, A., 2006. Sediment Cd and Mo accumulation in the oxygen-minimum zone off western Baja California linked to global climate over the past 52 kyr. Paleoceanography 21 (4), Pa4209. doi:10.1029/2005pa001239.
Duplessy, J.C., et al., 1989. AMS C-14 study of transient events and of the ventilation rate of the Pacific Intermediate Water during the last deglaciation. Radiocarbon 31 (3), 493–502.
Emerson, S., Bender, M., 1981. Carbon fluxes at the sediment–water interface of the deep-sea — calcium–carbonate preservation. J. Mar. Res. 39 (1), 139–162.
Fairbanks, R.G., 1989. A 17, 000-year glacio-eustatic sea-level record — influence of glacial melting rates on the Younger Dryas event and deep-ocean circulation. Nature 342 (6250), 637–642.
Fairbanks, R.G., et al., 2005. Radiocarbon calibration curve spanning 0 to 50,000 years BP based on paired Th-230/U-234/U-238 and C-14 dates on pristine corals. Quatern. Sci. Rev. 24 (16–17), 1781–1796.
Fine, R.A., et al., 2008. Decadal ventilation and mixing of Indian Ocean waters. Deep-Sea Res. I Oceanogr. Res. Pap. 55 (1), 20–37.
Fleitmann, D., et al., 2003. Holocene forcing of the Indian monsoon recorded in a stalagmite from Southern Oman. Science 300 (5626), 1737–1739.
Frank, M., et al., 1997. A 200 kyr record of cosmogenic radionuclide production rate and geomagnetic field intensity from ^{10}Be in globally stacked deep-sea sediments. Earth Planet. Sci. Lett. 149, 121–129.

Galbraith, E.D., et al., 2007. Carbon dioxide release from the North Pacific abyss during the last deglaciation. Nature 449 (7164), 890–894.

Ganeshram, R.S., Pedersen, T.F., Calvert, S.E., McNeill, G.W., Fontugne, M.R., 2000. Glacial–interglacial variability in denitrification in the world's oceans: Causes and consequences. Paleoceanography 15 (4), 361–376.

Goldstein, S.J., Lea, D.W., Chakraborty, S., Kashgarian, M., Murrell, M.T., 2001. Uranium-series and radiocarbon geochronology of deep-sea corals: implications for Southern Ocean ventilation rates and the oceanic carbon cycle. Earth Planet. Sci. Lett. 193 (1–2), 167–182.

Gordon, A.L., Fine, R.A., 1996. Pathways of water between the Pacific and Indian oceans in the Indonesian seas. Nature 379 (6561), 146–149.

Gordon, A.L., Giulivi, C.F., Ilahude, A.G., 2003. Deep topographic barriers within the Indonesian seas. Deep-Sea Res. II-Top. Stud. Oceanogr. 50 (12–13), 2205–2228.

Grootes, P.M., Stuiver, M., 1997. Oxygen 18/16 variability in Greenland snow and ice with 10(-3)- to 10(5)-year time resolution. J. Geophys. Res.-Oceans 102 (C12), 26455–26470.

Hughen, K., et al., 2004. C-14 activity and global carbon cycle changes over the past 50,000 years. Science 303 (5655), 202–207.

Hughen, K., Southon, J., Lehman, S., Bertrand, C., Turnbull, J., 2006. Marine-derived C-14 calibration and activity record for the past 50,000 years updated from the Cariaco Basin. Quatern. Sci. Rev. 25 (23–24), 3216–3227.

Ivanochko, T.S., et al., 2005. Variations in tropical convection as an amplifier of global climate change at the millennial scale. Earth Planet. Sci. Lett. 235 (1–2), 302–314.

Jaccard, S.L., et al., 2009. Subarctic Pacific evidence for a glacial deepening of the oceanic respired carbon pool. Earth Planet. Sci. Lett. 277 (1–2), 156–165.

Jouzel, J., et al., 2007. Orbital and millennial Antarctic climate variability over the past 800,000 years. Science 317 (5839), 793–796.

Jung, S.J.A., Kroon, D., Ganssen, G., Peeters, F., Ganeshram, R., 2009. Enhanced Arabian Sea intermediate water flow during glacial North Atlantic cold phases. Earth Planet. Sci. Lett. 280 (1–4), 220–228.

Keeling, R.F., Stephens, B.B., 2001. Antarctic sea ice and the control of Pleistocene climate instability. Paleoceanography 16 (1), 112–131.

Keigwin, L.D., 2004. Radiocarbon and stable isotope constraints on Last Glacial Maximum and Younger Dryas ventilation in the western North Atlantic. Paleoceanography 19 (4), Pa4012. doi:10.1029/2004pa001029.

Keigwin, L.D., Schlegel, M.A., 2002. Ocean ventilation and sedimentation since the glacial maximum at 3 km in the western North Atlantic. Geochem. Geophys. Geosyst. 3, 1034. doi:10.1029/2001gc000283.

Keigwin, L.D., Lehman, S.J., Cook, M.S., 2006. Radiocarbon evidence for a benthic front near 3 km in the Glacial Pacific Ocean. Eos Trans. AGU 87 (52) Fall Meet. Suppl., Abstract PP44A-07.

Key, R.M., et al., 2004. A global ocean carbon climatology: results from Global Data Analysis Project (GLODAP). Glob. Biogeochem. Cycles 18 (4), Gb4031. doi:10.1029/2004gb002247.

Laj, C., et al., 2002. Geomagnetic field intensity, North Atlantic Deep Water circulation and atmospheric Delta C-14 during the last 50 kyr. Earth Planet. Sci. Lett. 200 (1–2), 177–190.

Loubere, P., Bennett, S., 2008. Southern Ocean biogeochemical impact on the tropical ocean: stable isotope records from the Pacific for the past 25,000 years. Glob. Planet. Change 63 (4), 333–340.

Luyten, J.R., Pedlosky, J., Stommel, H., 1983. The ventilated thermocline. J. Phys. Oceanogr. 13 (2), 292–309.

Mangini, A., et al., 2010. Deep sea corals off Brazil verify a poorly ventilated Southern Pacific Ocean during H2, H1 and the Younger Dryas. Earth Planet. Sci. Lett. 293 (3–4), 269–276.

Marchitto, T.M., Broecker, W.S., 2006. Deep water mass geometry in the glacial Atlantic Ocean: a review of constraints from the paleonutrient proxy Cd/Ca. Geochem. Geophys. Geosyst. 7, Q12003. doi:10.1029/2006gc001323.

Marchitto, T.M., Lehman, S.J., Ortiz, J.D., Fluckiger, J., van Geen, A., 2007. Marine radiocarbon evidence for the mechanism of deglacial atmospheric CO2 rise. Science 316 (5830), 1456–1459.

Martinez, P., Robinson, R.S., 2010. Increase in water column denitrification during the last deglaciation: the influence of oxygen demand in the eastern equatorial Pacific. Biogeosciences 7 (1), 1–9.

McCarthy, M.C., Talley, L.D., 1999. Three-dimensional isoneutral potential vorticity structure in the Indian Ocean. J. Geophys. Res.-Oceans 104 (C6), 13251–13267.

McCartney, M.S., 1977. Subantarctic mode water. In: Angel, M.V. (Ed.), A Voyage of Discovery: George Deacon 70th Anniversary Vol., Deep-Sea Res. (Suppl.). Pergamon, pp. 103–119.

McManus, J.F., Francois, R., Gherardi, J.M., Keigwin, L.D., Brown-Leger, S., 2004. Collapse and rapid resumption of Atlantic meridional circulation linked to deglacial climate changes. Nature 428 (6985), 834–837.

McNichol, A.P., Gagnon, A.R., Jones, G.A., Osborne, E.A., 1992. Illumination of a black box — analysis of gas composition during graphite target preparation. Radiocarbon 34 (3), 321–329.

Meese, D.A., et al., 1997. The Greenland Ice Sheet Project 2 depth-age scale: methods and results. J. Geophys. Res.-Oceans 102 (C12), 26411–26423.

Monnin, E., et al., 2001. Atmospheric CO2 concentrations over the last glacial termination. Science 291 (5501), 112–114.

Muscheler, R., et al., 2004. Changes in the carbon cycle during the last deglaciation as indicated by the comparison of Be-10 and C-14 records. Earth Planet. Sci. Lett. 219 (3–4), 325–340.

Nadeau, M.-J., et al., 2001. Carbonate ^{14}C background: does it have multiple personalities? Radiocarbon 43 (2A), 169–176.

Ninnemann, U.S., Charles, C.D., 1997. Regional differences in Quaternary Subantarctic nutrient cycling: link to intermediate and deep water ventilation. Paleoceanography 12 (4), 560–567.

Okazaki, Y., et al., 2010. Deepwater formation in the North Pacific during the last glacial termination. Science 329 (5988), 200–204.

Olson, D.B., Hitchcock, G.L., Fine, R.A., Warren, B.A., 1993. Maintenance of the low-oxygen layer in the central Arabian Sea. Deep-Sea Res. II Top. Stud. Oceanogr. 40 (3), 673–685.

Oppo, D.W., Fairbanks, R.G., 1987. Variability in the deep and intermediate water circulation of the Atlantic Ocean during the past 25,000 years — Northern Hemispere modulation of the Southern Ocean. Earth.Planet. Sci. Lett. 86 (1), 1–15.

Ortiz, J.D., et al., 2004. Enhanced marine productivity off western North America during warm climate intervals of the past 52 ky. Geology 32 (6), 521–524.

Pahnke, K., Zahn, R., 2005. Southern hemisphere water mass conversion linked with North Atlantic climate variability. Science 307 (5716), 1741–1746.

Pahnke, K., Goldstein, S.L., Hemming, S.R., 2008. Abrupt changes in Antarctic Intermediate Water circulation over the past 25,000 years. Nat. Geosci. 1 (12), 870–874.

Peng, T.H., Broecker, W.S., 1984. The impacts of bioturbation on the age difference between benthic and planktonic foraminifera in deep-sea sediments. Nucl. Instrum. Methods Phys. Res. B-Beam Interact. Mater. Atoms 5 (2), 346–352.

Pichevin, L., Bard, E., Martinez, P., Billy, I., 2007. Evidence of ventilation changes in the Arabian Sea during the late Quaternary: implication for denitrification and nitrous oxide emission. Glob. Biogeochem. Cycles 21 (4), Gb4008. doi:10.1029/2006gb002852.

Pourmand, A., Marcantonio, F., Bianchi, T.S., Canuel, E.A., Waterson, E.J., 2007. A 28-ka history of sea surface temperature, primary productivity and planktonic community variability in the western Arabian Sea. Paleoceanography 22 (4), Pa4208. doi:10.1029/2007pa001502.

Reimer, P.J., et al., 2004. IntCal04 terrestrial radiocarbon age calibration, 0–26 cal kyr BP. Radiocarbon 46 (3), 1029–1058.

Reimer, P.J., et al., 2009. Intcal09 and Marine09 radiocarbon age calibration curves, 0–50,000 years cal BP. Radiocarbon 51 (4), 1111–1150.

Rickaby, R.E.M., Elderfield, H., 2005. Evidence from the high-latitude North Atlantic for variations in Antarctic intermediate water flow during the last deglaciation. Geochem. Geophys. Geosyst. 6, Q05001. doi:10.1029/2004gc000858.

Robinson, L.F., van de Flierdt, T., 2009. Southern Ocean evidence for reduced export of North Atlantic Deep Water during Heinrich event 1. Geology 37 (3), 195–198.

Robinson, L.F., et al., 2005. Radiocarbon variability in the western North Atlantic during the last deglaciation. Science 310 (5753), 1469–1473.

Robinson, R.S., Martinez, P., Pena, L.D., Cacho, I., 2009. Nitrogen isotopic evidence for deglacial changes in nutrient supply in the eastern equatorial Pacific. Paleoceanography 24, Pa4213. doi:10.1029/2008pa001702.

Rohling, E.J., Zachariasse, W.J., 1996. Red Sea outflow during the last glacial maximum. Quatern. Int. 31, 77–83.

Saenko, O.A., Weaver, A.J., Gregory, J.M., 2003. On the link between the two modes of the ocean thermohaline circulation and the formation of global-scale water masses. J. Climate 16 (17), 2797–2801.

Schulte, S., Rostek, F., Bard, E., Rullkotter, J., Marchal, O., 1999. Variations of oxygen-minimum and primary productivity recorded in sediments of the Arabian Sea. Earth Planet. Sci. Lett. 173 (3), 205–221.

Schulz, H., von Rad, U., Erlenkeuser, H., 1998. Correlation between Arabian Sea and Greenland climate oscillations of the past 110,000 years. Nature 393 (6680), 54–57.

Shackleton, N.J., et al., 1988. Radiocarbon age of Last Glacial Pacific deep-water. Nature 335 (6192), 708–711.

Sigman, D.M., Boyle, E.A., 2000. Glacial/interglacial variations in atmospheric carbon dioxide. Nature 407 (6806), 859–869.

Sijp, W.P., England, M.H., 2006. Sensitivity of the Atlantic thermohaline circulation and its stability to basin-scale variations in vertical mixing. J. Climate 19 (21), 5467–5478.

Sikes, E.L., Samson, C.R., Guilderson, T.P., Howard, W.R., 2000. Old radiocarbon ages in the southwest Pacific Ocean during the last glacial period and deglaciation. Nature 405 (6786), 555–559.

Sinha, A., et al., 2005. Variability of Southwest Indian summer monsoon precipitation during the Boiling-Allerod. Geology 33 (10), 813–816.

Skinner, L.C., Shackleton, N.J., 2004. Rapid transient changes in northeast Atlantic deep water ventilation age across Termination I. Paleoceanography 19 (2).

Skinner, L.C., Fallon, S., Waelbroeck, C., Michel, E., Barker, S., 2010. Ventilation of the deep Southern Ocean and deglacial CO_2 rise. Science 328, 1147–1151.

Sloyan, B.M., Rintoul, S.R., 2001. Circulation, renewal, and modification of Antarctic mode and intermediate water. J. Phys. Oceanogr. 31 (4), 1005–1030.

Spero, H.J., Lea, D.W., 2002. The cause of carbon isotope minimum events on glacial terminations. Science 296 (5567), 522–525.

Stott, L., Southon, J., Timmermann, A., Koutavas, A., 2009. Radiocarbon age anomaly at intermediate water depth in the Pacific Ocean during the last deglaciation. Paleoceanography 24, Pa2223. doi:10.1029/2008pa001690.

Stuiver, M., Polach, H.A., 1977. Reporting of C-14 data — discussion. Radiocarbon 19 (3), 355–363.

Swallow, J.C., 1984. Some aspects of the physical oceanography of the Indian Ocean. Deep-Sea Res. A Oceanogr. Res. Pap. 31 (6–8), 639–650.

Talley, L.D., 1996. Antarctic intermediate water in the South Atlantic. In: Wefer, G., Berger, W.H., Siedler, G., Webb, D.J. (Eds.), The South Atlantic: Present and Past Circulation. Springer-Verlag, Berlin Heidelberg, pp. 219–238.

Talley, L.D., 1999. Some aspects of ocean heat transport by the shallow, intermediate and deep overturning circulations. Mechanisms of global climate change at millennial time scales.: Geophysical Monograph. American Geophysical Union, Washington, DC, pp. 1–22.

Talley, L.D., Sprintall, J., 2005. Deep expression of the Indonesian Throughflow: Indonesian Intermediate Water in the South Equatorial Current. J. Geophys. Res.-Oceans 110 (C10), C10009. doi:10.1029/2004jc002826.

Toggweiler, J.R., 1999. Variation of atmospheric CO2 by ventilation of the ocean's deepest water. Paleoceanography 14 (5), 571–588.
Toggweiler, J.R., Dixon, K., Broecker, W.S., 1991. The Peru upwelling and the ventilation of the South Pacific thermocline. J. Geophys. Res.-Oceans 96 (C11), 20467–20497.
Wang, Y.J., et al., 2001. A high-resolution absolute-dated Late Pleistocene monsoon record from Hulu Cave, China. Science 294 (5550), 2345–2348.
Watson, A.J., Naveira Garabato, A.C., 2006. The role of Southern Ocean mixing and upwelling in glacial–interglacial atmospheric CO2 change. Tellus Ser. B-Chem. Phys. Meteorol. 58 (1), 73–87.
Wyrtki, K., 1973. Physical oceanography of the Indian Ocean. In: Zeirzscker, B. (Ed.), The Biology of the Indian Ocean. Springer, New York, pp. 18–36.
You, Y.Z., 1998. Intermediate water circulation and ventilation of the Indian Ocean derived from water-mass contributions. J. Mar. Res. 56 (5), 1029–1067.
Zahn, R., Pedersen, T.F., 1991. Late Pleistocene evolution of surface and mid-depth hydrography at the Oman Margin: planktonic and benthic isotope records at Site 724. In: Prell, W.L., Niitsuma, N. (Eds.), Proc. ODP, Scientific Results. Ocean Drilling Program, College Station, TX, pp. 291–308.